Title

Upscaling of Regional Scale Transport Under Transient Conditions: Evaluation of the Multirate Mass Transfer Model

Journal

Water Resources Research, 55(7)

ISSN

0043-1397

Authors

Guo, Zhilin
Fogg, Graham E
Henri, Christopher V

Publication Date

2019-07-01

DOI

10.1029/2019wr024953

Peer reviewed

Water Resources Research

RESEARCH ARTICLE
10.1029/2019WR024953

Upscaling of Regional Scale Transport Under Transient Conditions: Evaluation of the Multirate Mass Transfer Model

Zhilin Guo[1,2], **Graham E. Fogg**[1], **and Christopher V. Henri**[1]

[1]Land, Air, and Water Resources, University of California, Davis, CA, USA, [2]School of Environmental Science and Engineering, Southern University of Science and Technology, Shenzhen, China

Key Points:
- We evaluated the abilities of multirate mass transfer models to represent solute transport under transient conditions
- The multirate mass transfer (MRMT) model fails to reproduce tailings observed for the heterogeneous scenario under transient conditions
- Failure of the MRMT model is due to temporal changes in mass flux between aquifer and aquitard materials when boundary conditions change

Supporting Information:
- Supporting Information S1

Correspondence to:
Z. Guo,
zlguo@ucdavis.edu

Citation:
Guo, Z., Fogg, G. E., & Henri, C. V. (2019). Upscaling of regional scale transport under transient conditions: evaluation of the multirate mass transfer model. *Water Resources Research*, *55*. https://doi.org/10.1029/2019WR024953

Received 28 FEB 2019
Accepted 23 MAY 2019
Accepted article online 3 JUN 2019

Abstract Regional scale transport models are needed to support the long-term evaluation of groundwater quality and to develop management strategies aiming to prevent serious groundwater degradation. The purpose of this study is to evaluate the capacity of a previously developed upscaling approach to adequately describe the main solute transport processes, including the capture of late-time tails under changing boundary conditions. Potential factors that impact the performance of upscaling methods, including temporal variations in mass transfer rates and mass distributions, were investigated. Advective-dispersive contaminant transport in a 3-D heterogeneous domain was simulated and used as a reference solution. The equivalent transport under homogeneous flow conditions was then evaluated by applying the multirate mass transfer (MRMT) model. The random walk particle tracking method was used to solve the solute transport for heterogeneous and homogeneous MRMT scenarios under steady state and transient conditions. The results indicate that the MRMT model can capture the tails satisfactorily for plumes transported with ambient steady state flow fields at all studied scales using the same parameters. However, when the boundary conditions change in either local, plume, or regional scale, the mass transfer model calibrated for transport under steady state conditions cannot accurately reproduce the tailings observed for the heterogeneous scenario. The deteriorating impacts of transient boundary conditions on the upscaled model are more significant for regions where the flow fields are dramatically affected, which highlights the poor applicability of the MRMT approach for complex field settings. This finding also has implications for the suitability of other potential upscaling approaches.

1. Introduction

The declining groundwater quality caused by the chemicals and pathogens from agriculture and urban use, such as nitrate, pesticides, and salts, in intensely irrigated alluvial basins has been a major concern globally (e.g., Anastasiadis, 2004; Chae et al., 2004; Nativ, 2004; Nolan et al., 2002; Vengosh et al., 2002; Zektser & Everett, 2004; Zhang et al., 2006). Previous studies conducted on groundwater age and age dispersion (e.g., Fogg et al., 1999; Tompson et al., 1999; Weissmann et al., 2002) concluded that the mean age of the extracted groundwater in many wells is much older than the contaminant sources, which indicates the potential for the ongoing decline in groundwater quality during the coming decades and centuries (Fogg & LaBolle, 2006). The deterioration of groundwater quality will further impact the economic and social fabric that depend on those resources (e.g., Nativ, 2004). In this context, long-term (multidecadal) data and models on groundwater quality are necessary to evaluate the effects of current activities on groundwater quality, especially at intermediate and large depths (e.g., Fogg & LaBolle, 2006). For example, the long-term degradation of groundwater quality has been observed in the San Joaquin Valley, California, by studying an over four-decade trend of the nitrate concentration (Dubrovsky et al., 1998; Harter et al., 2012). However, these types of data are rare. Clearly, regional-scale groundwater quality management models that can adequately represent regional transport phenomena are needed to support the long-term evaluation of groundwater quality and to identify decadal time scale management strategies needed to reverse the ongoing degradation.

Regional groundwater quality management models must upscale the transport equation sufficiently to represent the effects of heterogeneity, including preferential flow in well-connected high-conductivity networks and mass transfer between the high- and low-conductivity media. The early arrivals of contaminants caused by the preferential flow and the asymptotical tails resulting from transport through low permeability

materials have been frequently observed, which significantly challenges long-term management (e.g., Bianchi et al., 2011; Brusseau & Guo, 2014; Brusseau et al., 2007, 2011; Dearden et al., 2013; Fogg et al., 2000; Fogg & LaBolle, 2006; Fogg & Zhang, 2016; Guo & Brusseau, 2017; LaBolle & Fogg, 2001; Matthieu et al., 2014; Seyedabbasi et al., 2012). Although the effects of heterogeneity can be simulated by explicitly including the spatial variability of hydraulic properties in the model, this approach is not feasible for most plume-scale contamination sites and is definitely not feasible for regional-scale models covering 10s to 100s of kilometer. As a result, the velocity fields from coarsely described regional flow models will typically be taken to represent the flow fields in these models. In this case, the advection-dispersion equation (ADE) is most likely to fail to reproduce the main transport behaviors due to heterogeneity. Accordingly, regional transport models that are capable of using regional velocity fields from flow models while also representing the appropriate transport phenomena are needed (Fogg & LaBolle, 2006).

In addition to representing the effects of subgrid-scale heterogeneity, regional water quality management models must be capable of representing transient boundary conditions and velocity fields. Indeed, we need not only to model the past degrading water quality caused by past land and water uses, but we also need to model the possible future changes in groundwater quality as a result of the changing contaminant sources and velocity fields caused by changes in recharge, groundwater and surface water interactions, and changing pumping rates and distributions. In other words, an upscaled regional model needs to (1) be as general as the model that accounts for a detailed representation of the heterogeneity and solves transport using the ADE and (2) be able to represent the effects of heterogeneity under transient flow as a result of temporally variable boundary conditions.

For example, consider a typically heterogeneous alluvial aquifer system consisting of stratified interbeds ranging from sands to clays. Although such deposits commonly function as integrated aquifer systems owing to the good connectivity of the sands (e.g., Belitz et al., 1993; Carle et al., 1998; Fogg, 1986; Fogg & Zhang, 2016; Weissmann et al., 2002), horizontal stratification can result in a substantially lower vertical effective hydraulic conductivity (K) compared to the horizontal K owing to the presence of numerous clay or silt beds. The ambient, horizontal hydraulic gradients in such systems are commonly on the order of 10^{-3}, yet the vertical hydraulic gradients can become more than one hundred-fold larger due to local effects, for example, a pumping well installed to extract a plume or regional effects of the simultaneous recharge from the surface and pumping of wells at depth. Clearly, these effects may significantly change the mass fluxes of solutes moving between the aquifer and aquitard sediments, and any reliable transport modeling method should be capable of representing such changes.

It is noteworthy that very few models have been produced that simulate pump-and-treat (PAT) remediation accurately without explicitly modeling all of the aquifer and aquitard interbeds that result in both the preferential flow and the late-time tails that can lead to decades-long PAT operations as well as PAT rebound (Guo & Brusseau, 2017; LaBolle & Fogg, 2001; Zhang & Brusseau, 1999). Upscaled transport modeling methods are needed that are capable of representing both forward plume movement under quasi-steady conditions and plume recovery under PAT or regional water quality changes under different land and water management schemes.

Many studies on upscaling have been published in past decades (e.g., Cassiraga et al., 2005; Dagan, 1994; Dagan & Lessoff, 2001; Fernàndez-Garcia et al., 2009; Fernàndez-Garcia & Gómez-Hernández, 2007; Fleckenstein & Fogg, 2008; Li et al., 2011; Renard & de Marsily, 1997; Rubin et al., 1999; Sanchez-Vila et al., 2006; Scheibe & Yabusaki, 1998; Wen & Gómez-Hernández, 1996; Zhou et al., 2010). Most of these studies have focused on upscaling the K field and have shown good preservation of the flows and heads. However, fewer efforts have been focused on upscaling transport processes (e.g., Cassiraga et al., 2005; Dagan, 1994; Fernàndez-Garcia et al., 2009; Fernàndez-Garcia & Gómez-Hernández, 2007; Li et al., 2011; Scheibe & Yabusaki, 1998; Willmann et al., 2008). It has been shown that models using flow upscaling approaches often fail to reproduce solute transport behaviors (e.g., Cassiraga et al., 2005; Dagan, 1994; Scheibe & Yabusaki, 1998).

To overcome the inability to represent non-Fickian or nonergodic behaviors, nonlocal methods have been developed. Among them, we can cite the continuous time random walk (CTRW; Berkowitz & Scher, 1995, 1998; Berkowitz et al., 2006), fractional ADEs (fADEs; Benson et al., 2000a, 2000b), multirate mass transfer (MRMT; Haggerty & Gorelick, 1995; Harvey & Gorelick, 2000; Silva et al., 2009), and memory

Table 1
Hydraulic Conductivity, K, and Porosity of the Four Hydrofacies for the Heterogeneous Simulations

			Direction and mean length		
Hydrofacies	K, m/d	Porosity	Strike (m)	Dip (m)	Vertical (m)
Gravel	124	0.25	360	500	9.6
Sand	45	0.25	200	265	8.6
Silt	3	0.25	380	350	13.8
Clay	0.00013	0.37	880	700	16.9

functions (Carrera et al., 1998; Carrera & Neuman, 1986). These nonlocal methods have displayed good potentials in reproducing complex transport behaviors but have only been tested under conditions where the flow fields are relatively simple and the boundary conditions are steady (e.g., Benson et al., 2001; Berkowitz et al., 2006; Cortis & Berkowitz, 2005; Harvey & Gorelick, 2000; Pedretti et al., 2014; Willmann et al., 2008; Zhang et al., 2007; Zinn & Harvey, 2003).

Importantly, methods such as MRMT, fADE, or CTRW show promise as means of upscaling transport, yet we are not aware of any tests of these methods for conditions other than steady state, forward plume movement. Although one might not expect that such methods would be capable of representing some of the transient scenarios mentioned above, where there are significant changes in the hydraulic gradients and mass fluxes between aquifers and aquitards, we believe it is important to test the performance of these methods to ascertain their general range of applicability under both steady and transient conditions. We hope this study will help refresh the discussion on how transport modeling methods need to continue to be improved to better address modern groundwater contamination problems (Fogg & Zhang, 2016).

This study investigates the performance of the MRMT method in describing solute transport, including representation of the late-time tails when the boundary conditions change. The possible factors explaining the performance of the MRMT method, such as variable flow fields and mass distributions, are explored. The local-scale impact was investigated by studying the plume transport across control planes located at different locations and a scenario in which regional-scale changes of the boundary conditions were applied, such as changes in recharge and flow fields due to extensive pumping. The MRMT method coupled with a random walk particle tracking (RWPT) code was applied for demonstration in this study. Although this work focuses on the MRMT method, our results provide insights into the possible limitations of other upscaling methods under transient conditions in heterogeneous aquifer systems.

2. Methods

In this study, 3-D heterogeneous domains were generated using a geostatistical method that is described in the next section. Groundwater flow and solute transport were simulated for fully heterogeneous domains under both steady state and transient conditions. Then, the groundwater flow and transport were upscaled and simulated under steady state and transient conditions. These processes will be discussed in detail in the following sections.

2.1. Heterogeneous Model

2.1.1. Geostatistical Simulation of the Heterogeneity

The computer program T-PROGS, which is based on a transition probability–Markov chain random-field approach described by Carle and Fogg (1996, 1997), Carle (1997), and Carle et al. (1998), was used to generate 3-D heterogeneous domains. The hydrofacies categories are identified by interpretation of the well logs collected from sites. Transition probabilities are measured and used to conditionally simulate realizations of hydrostratigraphy for each depositional direction (strike, dip, and vertical) and to generate 3-D realizations of random fields. In this study, 245 geological boreholes collected from the Tucson International Airport Area (TIAA) Superfund site (Zhang & Brusseau, 1999) were interpreted and categorized into four hydrofacies: clay (42.4%), silty sand (17.7%), sand (19.6%), and gravel (20.3%). The vertical lengths were determined directly from the borehole logs, whereas the strike and dip lengths were estimated through both analysis of the data and geologic interpretation (Carle et al., 1998; Carle & Fogg, 1997). The mean lengths of the four hydrofacies in the dip, strike, and vertical directions are summarized in Table 1. Based on the resulting Markov chain model of the transition probability, geostatistical conditional realizations were generated on a grid of 250 (strike) × 250 (dip) × 70 (vertical) nodes with a 20.0 m × 20.0 m × 1.0 m spacing. The top of the generated domain coincides with the water table. More details on the domain generation are discussed in Guo et al. (2019). Ten realizations were generated to perform the analysis. One of the realizations is shown in Figures 1 and S1 in the supporting information. The connectivity, herein defined as the binary condition of whether the coarse facies fully percolates in the x, y, or z direction, was calculated using a code that

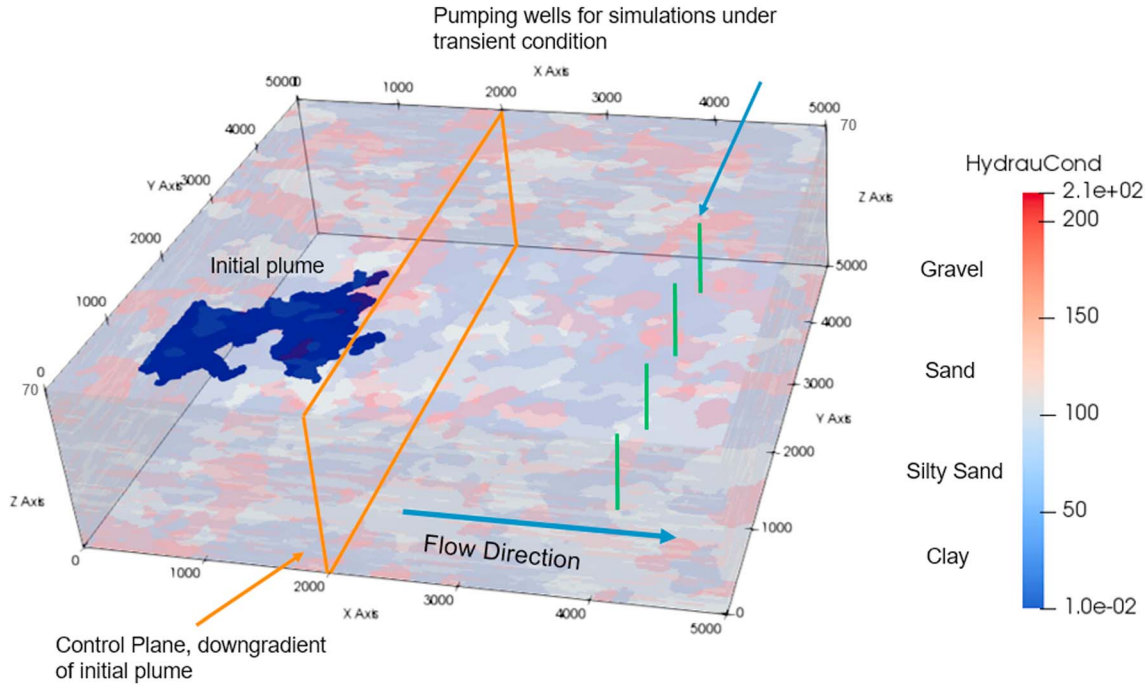

Figure 1. Heterogeneous domain for realization #1 and conceptual model setup.

searches for connectivity bodies and neighbors for each hydrofacies. In each realization, the coarse aquifer facies comprised 39.9% of the system containing sands or gravels, which were fully interconnected or percolated in all three dimensions. As a result, the overall transport behaviors, such as the early arrival due to preferential flow and late-time tailing, did not differ appreciably from realization to realization as illustrated in Figure 2. For example, the variance for the mean travel times of particles among 10 realizations reaching the control plane located at x = 4,000 m is approximately 0.58 years and the standard deviation is 0.76 years. This result is consistent with the findings of LaBolle and Fogg (2001). Therefore, we concluded that it was not necessary to perform a full stochastic analysis with an extensively large number of realizations.

2.1.2. Groundwater Flow Model

Groundwater flow was simulated using MODFLOW, a 3-D numerical (finite difference) groundwater flow model (McDonald & Harbaugh, 1988; Harbaugh et al., 2000) using the same grid as that of the geostatistical model. General head boundaries were used along the west and east borders of the domain, with a natural gradient (0.001) inducing lateral groundwater flow from west to east. The north, south, bottom, and top are no-flow boundaries. No vertical gradient was imposed in the boundary conditions. Spatially variable Ks and porosities are assigned to individual cells according to the categories of hydrofacies for the corresponding cells in the geostatistical domain (Table 1). The K and porosity for each hydrofacies used in the model were determined according to the information generated from geologic borehole logs, pumping tests, and historic data collected for the TIAA Superfund site (Zhang & Brusseau, 1999).

2.1.3. Solute Transport Model

The solute transport problem was solved using the code RW3D that solves advection, dispersion and multirate mass transfer using the RWPT approach (Fernàndez-Garcia et al., 2005; Henri & Fernàndez-Garcia, 2014; Henri & Fernàndez-Garcia, 2015; Salamon et al., 2006). The governing equation for advective-dispersive transport is given by the following:

$$\theta R\frac{\partial c}{\partial t} = \nabla\cdot(\theta \mathbf{D}\nabla c) - \nabla\cdot(\mathbf{q}c) \quad (1)$$

where $\mathbf{q}$ (L/T) is the groundwater flux, $\mathbf{D}$ (L^2/T) is the dispersion tensor, θ (dimensionless) is the porosity, c (M/L^3) is the aqueous concentration, and R (dimensionless) is the retardation factor.

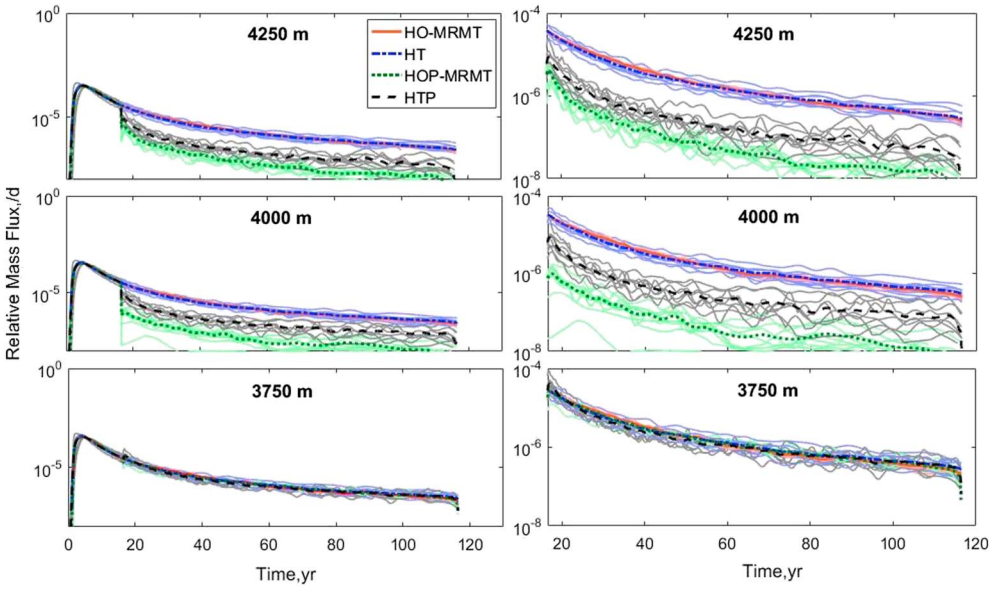

Figure 2. Breakthrough curves for 10 realizations and the mean of these realizations (bold lines) generated for control planes at different locations: x = 3,750, 4,000, and 4,250 m. HO-MRMT and HT refer to the homogeneous and heterogeneous results under steady state conditions, respectively. HOP-MRMT and HTP refer to the homogeneous and heterogeneous results under transient conditions, respectively. The figures on the right side magnify the tails.

The conceptual foundation of the code RW3D, which implements the RWPT methodology, was discussed by Fernàndez-Garcia et al. (2005). Particles are moved by advection according to their location in the flow field and by dispersion by introducing a random term in the RWPT algorithm (e.g., Boso et al., 2012; Salamon et al., 2006) as follows:

$$\mathbf{x}_{t+dt} = \mathbf{x}_t + \mathbf{A}(\mathbf{x}_t, t)dt + \mathbf{B}(\mathbf{x}_t, \mathrm{dt})\cdot\boldsymbol{\xi}(\mathrm{t})\sqrt{dt} \tag{2}$$

$$\mathbf{A}(t) = \frac{\mathbf{q_p}}{\theta R} \tag{3}$$

$$\mathbf{B}\cdot\mathbf{B}^t = \frac{2\mathbf{D}}{R} \tag{4}$$

where $\mathbf{x}_t$ is the particle position at time t; vector $\mathbf{A}$ and matrix $\mathbf{B}$ are related to the advection and the dispersion displacements of a particle, respectively; $\boldsymbol{\xi}$ is a vector of independent and normally distributed random variables characterized by a zero mean and a unit variance; and $\mathbf{q_p}$ (L/T) is the modified Darcy velocity, which is defined as $\mathbf{q_p} = \mathbf{q} + \nabla\cdot(\theta\mathbf{D})$. The dispersion tensor used here has the form given by Lichtner et al. (2002).

The longitudinal, transverse, and vertical dispersivities representing the grid-scale dispersion were set to 1.0, 0.1, and 0.01 m, respectively. To date, most of the dispersion in this system has been imparted by the geostatistically modeled heterogeneity. The aqueous diffusion coefficient was 7.6×10^{-5} m^2/day. This value resulted in an average Péclet number (Pe) of 0.03 for clay, which is determined as the ratio of the characteristic time for diffusion (t_D) and the time scale for advection (t_A). For a system with Pe greater than one, the system is considered an advective-dominant system since advection is faster than diffusion. For a system with Pe smaller than one, the system is diffusion dominant (Guswa & Freyberg, 2000). Therefore, the natural gradient flow in this study is a diffusion-dominant system. A retardation factor of 1.4 was applied. These parameters were determined based on the data for trichloroethene collected from the TIAA Superfund site (Zhang & Brusseau, 1999).

2.2. Upscaled Model

2.2.1. Effective Flow Field

The equivalent flow fields for the homogeneous simulations were generated by upscaling the heterogeneous K fields. The specified head boundaries were applied to two sides along the x axis of the domain and no-flow

Table 2
Mass Transfer Coefficient, Capacity Coefficient, and Damkohler Number for Each Immobile Zone

		Capacity coefficient	Mass transfer coefficient	Retardation factor	Damkohler number
Mobile zone		NA	NA	1.4	NA
Immobile zones	1	0.35	0.005	1.4	6.62
	2	0.45	0.003	1.4	4.26
	3	0.5	0.0005	1.4	0.74
	4	0.7	0.0001	1.4	0.17

boundaries to the other four bounds. For the heterogeneous case, a gradient of 0.001 was imposed across the domain. The equivalent K values along the x direction were computed based on the flow rates out of the downstream edges of the domains for the heterogeneous simulations using Darcy's equation. The equivalent Ks in the y and z directions were determined in the same way, using the flow rates leaving the side and bottom edges of the heterogeneous domain, respectively. The relative difference in flow between the homogeneous and heterogeneous cases was below 0.5%, indicating that the homogenous equivalent parameter preserves the average velocity and water balance observed in the heterogeneous case. For the transient conditions we simulated, the differences for the water budgets are also less than 1%, which shows that the flow field is preserved under the transient conditions.

2.2.2. Transport Upscaling

The MRMT model, which was used to upscale the heterogeneous transport model, has been described by Haggerty and Gorelick (1995) as follows:

$$\frac{\partial c_m}{\partial t} + \sum_{j=1}^{N_{im}} \beta_j \frac{\partial c_{im,j}}{\partial t} = \zeta(\mathrm{c}_m) \tag{5}$$

$$\frac{\partial c_{im,j}}{\partial t} = \frac{\alpha_j}{R_{im,j}} \left(\mathrm{c}_m - c_{im,j}\right) \tag{6}$$

where $\mathrm{c_m}$ ($\mathrm{M/L^3}$) is the aqueous concentration in the mobile zone; $\mathrm{c_{im}}$ ($\mathrm{M/L^3}$) is the concentration in the jth immobile zone; $\mathrm{N_{im}}$ is the number of distinct immobile zones; $\alpha_j$is the first-order mass transfer rate between the mobile zone and jth immobile zone; and $\zeta(\mathrm{c}_m)$ is the transport operator of the mobile concentrations defined by the following:

$$\zeta(\mathrm{c}_m) = \nabla \cdot \left(\frac{\mathbf{D}\nabla c_m}{R_m}\right) - \nabla \cdot \left(\frac{\mathbf{q} c_m}{\theta_m R_m}\right), \tag{7}$$

where $\mathrm{R_m}$ (dimensionless) is the retardation factor in the mobile domain. The total capacity β is the ratio of the total contaminant mass in the immobile zone to the total mass in the mobile zone at equilibrium and is calculated by summing the capacity ratios of all immobile domains, that is,

$$\beta = \sum_{j=1}^{N_{im}} \beta_j = \sum_{j=1}^{N_{im}} \frac{R_{im,j}\theta_{im,j}}{R_m \theta_m} \tag{8}$$

where θ_m (dimensionless) is the porosity of the mobile zone; $\theta_{im,j}$(dimensionless) is the porosity of the jth immobile zone ($j = 1..., \mathrm{N_{im}}$); and $\mathrm{R_{im,j}}$ (dimensionless) is the retardation factor of the jth immobile domain ($j = 1..., \mathrm{N_{im}}$). The total capacity was determined according to the ratio of the total pore volume of clay and silty sand in the first realization of the heterogeneous K field, where advection is minimal and can therefore be assumed as equivalent to the total volume of the immobile domain, to the total pore volume of the other hydrofacies, where advection is dominant. Values are given in Table 2.

The mass transfer coefficient and capacity coefficient for each immobile zone were determined by fitting the breakthrough curves (BTCs) generated for the control planes located at 4,000 m for the homogeneous simulations to the corresponding BTCs for the heterogeneous simulations conducted in the domain of realization #1. As all of the realizations were generated based on the same geological data, it was assumed that the physically based parameters should not vary among realizations. Therefore, the determined mass transfer coefficients and capacity coefficients fitted for realization #1 were used for the other realizations. The results presented below are for realization #2. The dispersivities and diffusion coefficients were set as the same as those used for the heterogeneous simulations since we assumed that the MRMT model would reproduce the macrodispersion resulting from the spatial variability in K. A porosity of 0.05 for the mobile zone and retardation factor of 1.4 were used to match the arrival times of the solute on the BTC and the center of the plume with those of the heterogeneous simulations. The low porosity used here also accounts for the

Table 3
Summary of the Simulated Scenarios

ID	Scenario	Description	Result representation
S1	Steady state	Purely horizontal flow with natural gradient for 120 years	HO-MRMT, HT[1]
S2	Transient	Two stress periods: first, horizontal flow for 16.4 years and, second, pumping initiated	HOP-MRMT, HTP[2]
S3	Transient	Two stress periods: first, horizontal flow for 16.4 years and, second, predominant vertical flow by increasing the vertical gradient regionally	HOTR-MRMT, HTTR[3]
S4	Rebound test 1	Three stress periods: first, horizontal flow for 16.4 years; second, pumping for 20 years; and third, pumping ceased and flow with natural gradient	HOP-MRMT-rebound, HTP-rebound[4]
S5	Rebound test 2	Four stress periods: first, horizontal flow for 16.4 years; second, pumping for 20 years; third, pumping ceased for 10 days; and fourth, pumping restarted	HOP-rebound, HTP-rebound[5]

[1]Homogeneous simulation with multirate mass transfer and heterogeneous simulation under steady state conditions. [2]Homogeneous simulation with multirate mass transfer and heterogeneous simulation under transient conditions for the pumping scenario. [3]Homogeneous simulation with multirate mass transfer and heterogeneous simulation under transient conditions for the regional flow change scenario. [4]Homogeneous simulation with multirate mass transfer and heterogeneous simulation under transient conditions for rebound test 1. [5]Homogeneous simulation with multirate mass transfer and heterogeneous simulation under transient conditions for rebound test 2.

effective porosity of the upscaled heterogeneous system, in which only approximately 40% of the system consists of aquifer materials.

2.3. Simulations

Both steady state and transient flow were simulated for heterogeneous and upscaled homogeneous scenarios (Table 3). The total simulation time for steady state flow (S1 in Table 3) was 120 years. Two stress periods were simulated for transient flow (S2 in Table 3). For the first stress period, groundwater flowed from west to east, induced by a natural gradient for 16.4 years, and the plume migrated via ambient steady state flow fields. During the second stress period, four wells located near $x = 3{,}900$ m (shown in Figure 1) started pumping for 100 years to represent the PAT remediation system. The total pumping rate was approximately one fourth of the total inflow discharge, which was able to capture a satisfactory amount of the downgradient plume without impacting the downgradient boundary. The simulations were conducted for heterogeneous domains first. An instantaneous input with an initial mass of 66,900 kg was placed in cells containing the gravel facies upgradient of the domain (Figure 1). Then, the homogeneous simulations were conducted in the equivalent flow fields described in section 2.2.4. The solute transport for homogeneous domains was simulated using the MRMT model with the upscaled parameters. To be consistent with the heterogeneous simulations, the same amount of mass was placed in the same location. Additional simulations were conducted with pumping rates that were increased by a factor of 3 for realization #1 to test the impact on transport with different radius of influence for both homogeneous and heterogeneous simulations. For all simulations, the solute mass flux was determined at a total of nine vertical control planes located at $x =$ 2,500, 3,000, 3,250, 3,500, 3,750, 4,000, 4,250, 4,500, and 4,750 m, corresponding to 5.3, 7.1, 8.0, 8.9, 9.8, 10.7, 11.6, 12.5, and 13.4 times, respectively, the mean length of 280m of the coarse hydrofacies (gravel and sand; Table 1). The BTCs plotted using the relative mass flux ($\boldsymbol{J}$) versus time were used to evaluate the performance of the MRMT model at different scales. An adaptive kernel density estimator method (Pedretti & Fernandez-Garcia, 2013) was used to reconstruct the BTCs to mitigate subsampling effects. The late-time slopes of the BTCs were determined based on the straight lines that were plotted on a log-log scale, $d\ (\log_{10} \boldsymbol{J})/d\ (\log_{10} \mathrm{t})$. The errors between the slopes for the heterogeneous and upscaled MRMT models were then calculated to quantitatively indicate the discrepancy.

To test the ability of the MRMT model to reproduce PAT remediation rebound, where concentrations recover rapidly after pumping is ceased and then restarted, two additional sets of simulations were produced with transient flow. In the first set (S4 in Table 2), pumping ceased after 20 years of extraction (in the second stress period), which was 36.4 years after the simulation started, and the boundary condition was changed back to the boundary condition in the first stress period. The mass fluxes across the control planes located at $x = 4{,}000$ m and $x = 4{,}250$ m were measured. Another set of rebound tests (S5 in Table 2) were

conducted by restarting extraction after pumping had ceased for 10 days in the first set of rebound tests, and the boundary condition was set the same as the boundary condition in the second stress period for transient flow. The BTCs were plotted using the concentrations collected from the extraction wells.

The nonergodicity effects in the heterogeneous simulations caused by local variations in the transport at scales smaller than the facies mean lengths are not considered to be a problem in this study because the transport is strongly influenced by the connectivity of the aquifer facies, which fully percolates in all three dimensions. Nevertheless, to help ensure that the results are not significantly affected by, for instance, the pumping wells being adjacent to locally idiosyncratic heterogeneous features, we also ran a simulation without pumping wells in which the changes in the regional flow field were regional rather than local (S3 in Table 2). The simulation was set up similarly as the transient scenario described above, with two stress periods. In the first stress period, we have ambient west-to-east groundwater flow for 16.4 ears with no vertical gradient. In the second stress period, the boundary conditions were changed by introducing a downward vertical gradient consistent with field conditions in which recharge, together with pumpage at depth, induces a downward component of flow. The recharge was applied at the top of the domain and the general head boundary at the bottom, which mimics the extensive pumping in the deep aquifer that can result in significant vertical flow at a large scale. A vertical gradient of 0.3 was simulated to represent the effects of simultaneous pumping at depth and recharge at the water table, resulting in an average Pe of 15 in the vertical direction and turning the system to an advective-dominant system. This magnitude of the vertical gradient would be representative in many areas of the Central Valley of California, where both heavy pumping and recharge from irrigation create strong vertical gradients with a range of 0.1 to 0.65 in the upper and middle portions of the aquifer system (Gailey, 2018; Styles & Burt, 1999).

3. Results

3.1. Performance of the MRMT Method Under Ambient Flow

The BTCs resulting from the transport simulations in the 10 heterogeneous realizations are plotted in Figure 2 and labeled as HT. Four immobile zones were required to be applied in the homogeneous MRMT (HO-MRMT) simulations to fit the BTCs resulting from the heterogeneous simulations. The mass transfer and capacity coefficients for each immobile zone are listed in Table 2. Values of the Damkohler number (Da_j), a dimensionless parameter describing the magnitude of the nonideal transport associated with mass transfer processes and characterizing the ratio of the mass transfer timescale to the advection timescale, are also listed in Table 2. For each immobile zone j, the Damkohler number can be calculated by the following:

$$Da_j = \left[\alpha_j\left(\beta_j + 1\right)R_m L\right]/v_x, \tag{9}$$

where v_x is the pore water velocity (L/T), which is calculated by the Darcy equation and the porosity of the mobile zone, and L is the domain length (L). The estimated Damkohler numbers are within the range of 0.01 and 100, which means that the concentration will be sensitive to the discharge rate and that a significant mass transfer effect is observed (Haggerty & Gorelick, 1995).

For the steady state conditions, the plume was moving forward with natural gradient flow. Long tails are observed from the BTCs for the heterogeneous simulations (HT in Figure 2), where the mass transfer between low- and high-K units has a significant effect. The upscaled equivalent model (HO-MRMT in Figure 2) was able to reproduce the tails of the BTCs generated for the heterogeneous simulations, which has also been demonstrated in previous studies (e.g., Haggerty & Gorelick, 1995; Harvey & Gorelick, 2000). As mass transfer coefficients were obtained from model results at the control planes at $x = 4{,}000$ m, the homogeneous simulation captured the tails perfectly (Figure S2) for the BTCs at this location. BTCs were also plotted using results from the control planes at other locations for the HO-MRMT case, which were also acceptably matched to the corresponding curves from the heterogeneous simulations (Figure S2). This result is consistent with the results presented in Haggerty et al. (2004), which showed that the mass transfer time is not correlated with the advection time for data collected in sorptive porous media. The minimal changes in the matches at different locations also indicate the negligible impacts arising from the scale and nonergodicity.

3.2. Performance of MRMT Under Transient Conditions

The BTCs for the pumping scenarios in both the fully heterogeneous case (HTP) and the upscaled homogeneous MRMT case (HOP-MRMT) are also shown in Figure 2. Reductions in the mass flux after the start of pumping at 16.4 years occurred in both simulations due to the large amount of mass extracted by pumping. As all mobile masses in the homogeneous MRMT domain were accessible to be extracted, while only the mass residing in the coarse materials in the heterogeneous domain was easily accessible, the mass flux for the homogeneous simulation (HOP-MRMT) dropped more than the mass flux for the heterogeneous simulation (HTP). The differences between the tails of the BTCs for the homogeneous MRMT and heterogeneous simulations are more pronounced downgradient of the extraction wells (at 4,000 and 4,250 m) compared to the upgradient area (at, e.g., 3,750 m). This phenomenon is also reflected in the calculated errors between the slopes of the tails for the homogeneous MRMT and heterogeneous simulation shown in Table S1. The errors become much larger, as high as −58%, for the simulations under transient flow conditions. In comparison, the errors of the steady state simulations are below 5%. For the control planes located downgradient of the wells, such as $x = 4{,}000$ m, the slope errors observed are larger than the errors observed at the planes located further away downgradient ($x = 4{,}250$ m and $x = 4{,}500$ m). After the start of pumping, the resulting Pe in 92% of the clay facies within the radius of influence was increased 1.2 to 10^6 times compared to the value of 0.03 for the natural gradient flow, resulting in the Pe for 73% of the clay facies within the radius of influence being larger than 1. Therefore, the system becomes advective dominant after pumping is started. The results of the simulations with higher pumping rates are presented in Figure S3. As larger radius of influence result from the increased pumping rates, the disparities of the mass flux between the homogeneous MRMT and heterogeneous simulations increase, and the impact expands further downgradient, that is, the difference in the mass flux at 4,500 m increases.

3.3. Performance of the MRMT Model Under Transient Conditions for the Rebound Tests

Figure 3 shows the mass flux changes at the control planes located at $x = 4{,}000$ m and $x = 4{,}250$ m for the rebound tests in which pumping was turned off after 20 years of extraction. For comparison, the mass flux changes for the corresponding scenarios under both steady state and transient conditions are also shown. Rebounds of the mass fluxes are observed for both the homogeneous MRMT and heterogeneous simulations but by greater amounts for the latter. In the heterogeneous case, the rebound rises above the mass flux for the steady state case at 36.4 years, which is apparently due to (a) a higher mass flux from the coarse to the fine materials during the pumping period and (b) a reversed flow direction after wells are turned off, leading to a greater transport of particles toward the control plane that were previously moving in the opposite direction due to pumping. Once the increased number of particles crosses the control plane causing the rebound, the mass flux overlaps with the mass flux observed for the steady state simulation, which is expected since the flow fields are identical, and therefore, the mass transfer coefficients calibrated under steady state conditions work well. The errors shown in Figure 3 for the mass flux between the MRMT and heterogeneous simulations are also reflected in the concentrations (Figure S4). The differences between the flow rates for the homogeneous MRMT and heterogeneous simulations are listed in Table S2. Figure S4 shows the change in concentration with time at $x = 4{,}250$ m. Therefore, the errors of the concentrations between the homogeneous MRMT and heterogeneous simulations are also 1–2 orders of magnitude under transient conditions, and the errors of the rebound are approximately half an order of magnitude.

The BTCs recorded at the extraction wells are presented in Figure 4. HOP-MRMT and HTP are the BTCs for the homogeneous MRMT and heterogeneous simulations with continuous pumping, respectively. The homogeneous MRMT simulation was not able to accurately represent the concentrations in the effluents from the wells obtained for the heterogeneous simulation until the concentration dropped by approximately 2 orders of magnitude (after approximately 40 years of pumping). The differences between the concentrations of the homogeneous MRMT and heterogeneous simulations are as large as a factor of 2 to 3. Figure 4b shows the BTCs for the rebound tests on a semilog scale. After pumping was resumed, the concentration of the heterogeneous simulation increased by approximately a factor of 2 and then dropped to the concentration level of the simulation with continuous pumping. The homogeneous MRMT model failed to represent this rebound, which reflects the failure of the MRMT method to reproduce the mobile-to-immobile zone mass fluxes occurring in the transient rebound case.

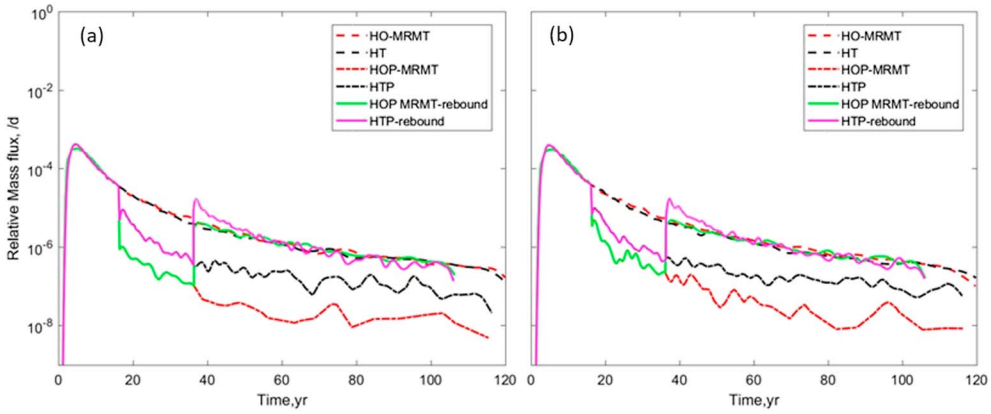

Figure 3. Breakthrough curves at the control planes located at x = 4,000 m (a) and x = 4,250 m (b) for the rebound test during which pumping was turned off after 20 years of extraction.

3.4. Contaminant Mass Distributions

The mass distributions within the domains under steady state conditions at different times are shown in Figures 5a and 5b for the homogeneous MRMT and heterogeneous cases, respectively. An uneven mass distribution is observed for the heterogeneous system as a result of the permeability spatial variability (Figure 5b), whereas the mass distribution in the homogeneous MRMT domain is, as expected, more uniform (Figure 5a). The mass distributions in the homogeneous MRMT and heterogeneous domains as a function of the distance at different times after pumping started are shown in Figure 6. Pumping was started after 16.4 years of ambient flow. The mass residing within the radius of influence (~300 to 400 m near the well locations) was more impacted than those at other locations. For the homogeneous simulation whose mass distribution was relatively uniform in the steady state, after pumping started, apparent mass decreases are observed within the radius of influence. In addition, more mass was retained near the upgradient source zone compared to the heterogeneous scenario at the same time because of retardation. An uneven mass distribution is also observed after pumping started, and more mass is retained at a distance of approximately 2,300 m due to the extensive presence of clay in the region.

Figure S5 shows the particle distributions after 6 years of plume migration under ambient flow for the homogeneous MRMT simulation and heterogeneous simulation. Relatively uniform distributions of particles are

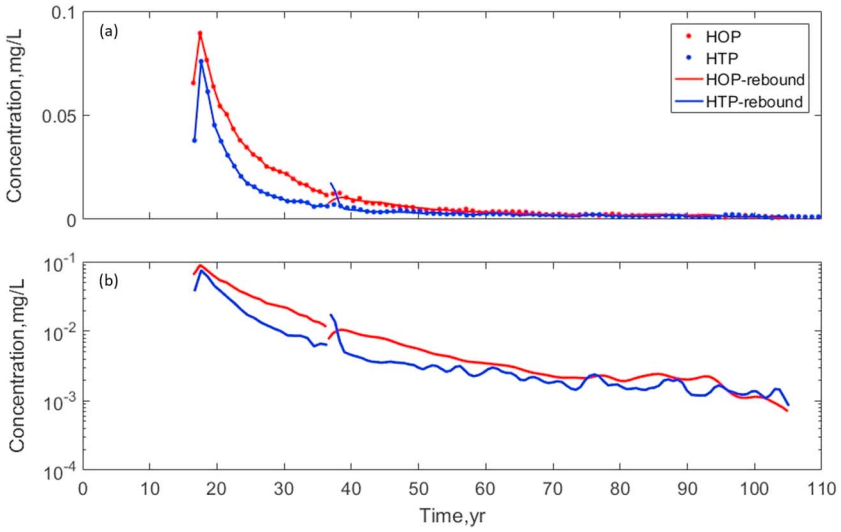

Figure 4. Time continuous concentrations measured from the extraction wells for the scenario with continuous pumping and the rebound test, where pumping was resumed after stopping extraction for 10 days following 20 years of continuous pumping: (a) normal scale and (b) semilog scale.

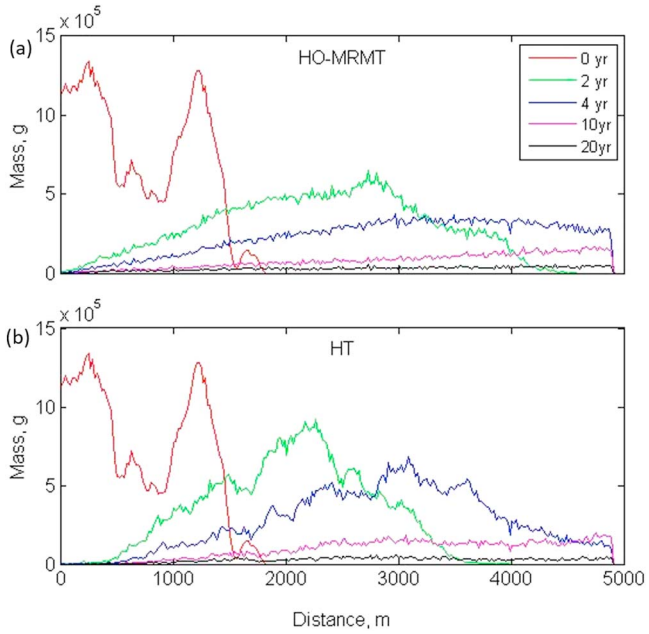

Figure 5. Mass distribution under steady state conditions at different time periods: (a) homogeneous MRMT simulation and (b) heterogeneous simulation. MRMT = multirate mass transfer.

observed for the homogeneous simulation, whereas for the heterogeneous simulation, the particles are distributed unevenly through the domain with a portion of the particles trapped within low permeability zones, while relatively rapid transport occurs in well-connected channels. These observations are consistent with the mass distributions depicted in Figures 5 and 6. The fact that the observed preferential transport and mass trapped in low permeability zones cannot be reproduced by the homogeneous MRMT model helps explain the failure of the MRMT model when applied under more general or transient conditions, which will be further discussed in the following section.

3.5. Maximum Concentrations

Figure 7 shows the maximum concentrations with the distance at different times for the homogeneous MRMT and heterogeneous simulations under steady state conditions. The concentration and mass held back at later times of the heterogeneous case show higher values in general compared with the results of the MRMT simulation, which shows lower concentrations and relatively uniform concentrations at later times. The results of the simulations with pumping started later are presented in Figure S6. Some oscillation is evident in Figure S6 due to declines in the particle numbers. Simulations with more particles would generate smoother solutions. Nevertheless, these results illustrate the general behavior that more spatially variable concentrations are observed for the heterogeneous case, whereas uniform low concentrations are observed for the homogeneous MRMT case.

Therefore, in regards to the local problem, MRMT models failed to capture the high concentrations observed in the heterogeneous simulations. However, in this case, the difference between the high concentrations of the heterogeneous simulation and the corresponding concentrations at the same locations of the homogeneous MRMT simulations are less than 1 order of magnitude. This result has implications for addressing different contaminants that have different regulatory contaminant levels.

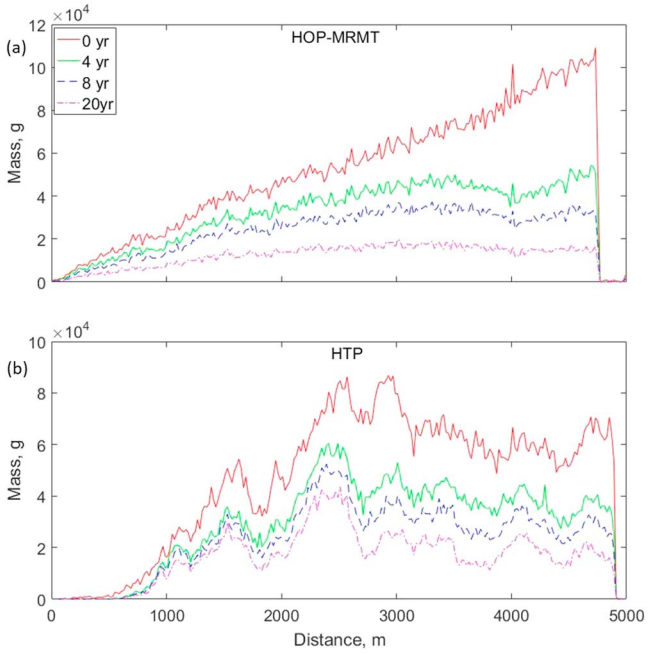

Figure 6. Mass distribution at different times after pumping started (after 0, 4, 8, and 20 years of pumping): (a) homogeneous MRMT simulation and (b) heterogeneous simulation. MRMT = multirate mass transfer.

4. Discussion

4.1. Reasons for the Failure of the MRMT Model Under Transient Conditions

The mismatches of the late-time slopes between the MRMT and heterogeneous simulations after changing the boundary conditions indicate a limitation of applying the MRMT method when the flow field is transient. This finding is consistent with previous studies whereby a concrete relationship between the aquifer and mathematical parameters can only be built for limited systems, such as a diffusion-dominant system (Carrera et al., 1998; Haggerty & Gorelick, 1995; Pedretti et al., 2014; Nkedi-Kizza et al., 1984), which indicates the possible failure of applying the MRMT method when the system changes from diffusion dominant to advection dominant or the opposite way. The non-Fickian transport, that is, the early- and late-time tails arise especially because of the strong heterogeneity, including the connectivity of the high-K media and the presence of substantial amounts of low-K media. As shown in Figures 2 and 3, the early arrivals observed in the BTCs are due to the high permeability zones, which percolate horizontally through the entire domain, and the late-time tails result from the slow mass transfer process through the extensive low permeability lenses in the domain. In most sedimentary alluvial systems, the high- and low-K media are in the form of laterally extensive, stratified

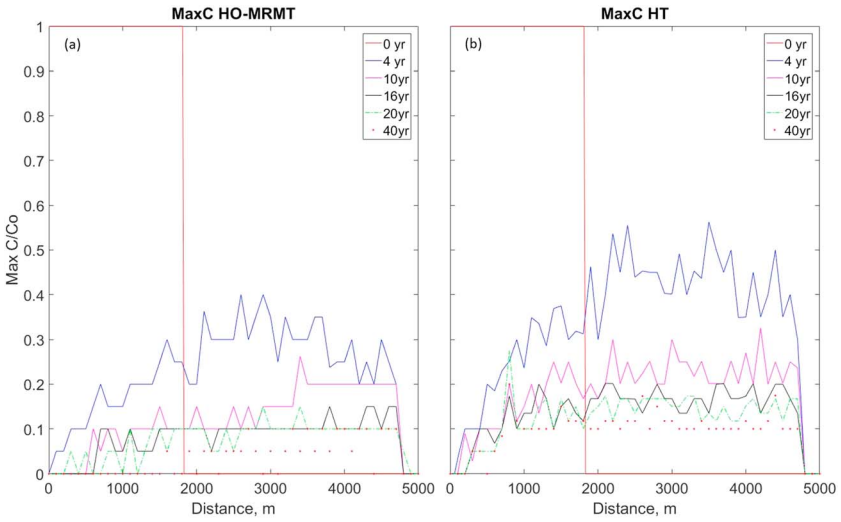

Figure 7. The maximum concentration with the distance at different time periods: (a) homogeneous MRMT simulation and (b) heterogeneous simulation. MRMT = multirate mass transfer.

sands/gravels, silts, and clays, with the latter commonly making up the majority of the systems as is the case for the study site in this work. The transport in these systems can be strongly affected by slow advective processes, which can change dramatically as the boundary conditions change. The simulated scenarios above, in which ambient plume migration is followed by transient changes in the flow system, present an effective test on the application of the non-Fickian method on non-Fickian transport with a transient boundary condition.

4.1.1. Perturbation of the Mass Transfer Caused by Variable Flow Fields

The mismatches in the tails between homogeneous the MRMT and heterogeneous simulations of transient scenario S2 are observed for the BTCs at all monitored control planes after pumping started (Figure 2); however, the degrees of the mismatches are different, which is more apparent for the control planes located downgradient of the wells than the wells located upgradient (e.g., Figure 2). The relative changes in the fluxes (from the steady state to the pumping regime) across the five control planes located within the radius of influence were calculated and listed in Table S2 for both the homogeneous MRMT and heterogeneous simulations. The changes in the total fluxes across all control planes located downgradient of the pumping wells are similar and so are the changes in the total fluxes across the control planes upgradient of the wells due to preservation of the water balance. However, the changes in the fluxes across the portion of the control planes located within the radius of influence of the pumping wells (identified by analyzing the drawdowns) show high disparities.

The calculated errors between the slopes of the tails for the homogeneous MRMT and heterogeneous simulation versus the percentage changes in the fluxes across the portion of the control planes located within the radius of influence for the 10 realizations are plotted in Figure 8. For the control planes located downgradient of the pumping wells, the flux directions reversed, resulting in negative percent change values. Overall, the slope errors for a given realization become larger as the change in the flux increases. The errors between the slopes are relatively high for the negative percentage changes in the fluxes (left side in Figure 8) due to the reversal of the flow direction, among which most of the errors are in the range of 5% to 40% and can be as high as 58.67%. Therefore, for the control planes located downgradient of the wells, such as x = 4,000 m, the slope errors observed are larger than the errors observed at the planes located further downgradient (x = 4,250 m and x = 4,500 m). On the other hand, the slope errors are relatively small for the cases with positive percentage changes in the fluxes (for the planes located upgradient of the wells, right side in Figure 8), as the changes in the flow field, where the main flow direction remains unchanged, are not as dramatic as the changes in the flow field downgradient of the wells. Therefore, relatively small changes in the tail slopes are observed between the homogeneous MRMT and heterogeneous simulations for the control planes located upgradient of the wells (x = 3,500 m and x = 3,750 m). The results highlight the

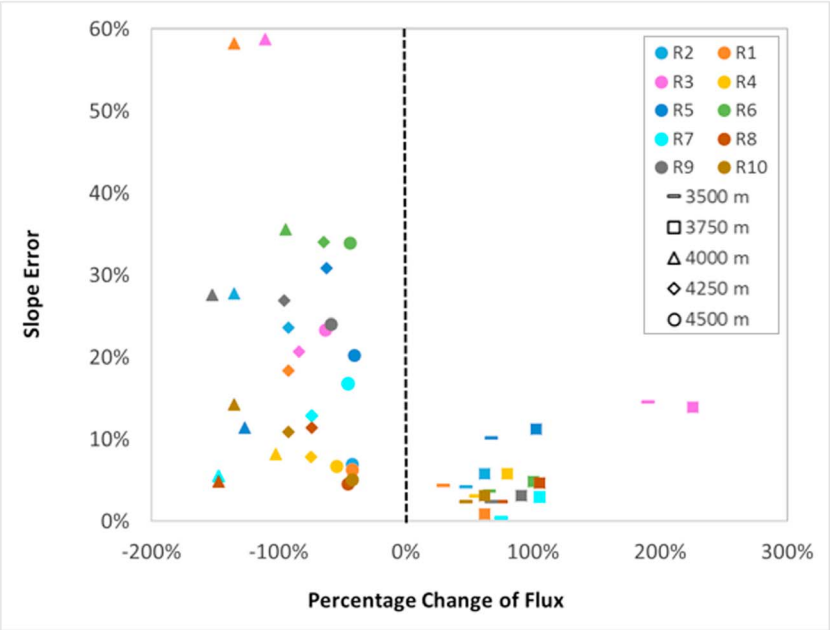

Figure 8. Errors between the slopes of the tails for the homogeneous and heterogeneous simulations versus the percentage changes in the fluxes across the control planes within the radius of influence for 10 realizations. A negative percentage change in the flux indicates a change in the flow direction.

importance of the changes in the fluxes induced by extractions on the performance of the MRMT approach in reproducing the tailings.

4.1.2. Misrepresentation of the Mass Distribution

The mass distributions throughout the domain are very different between the homogeneous MRMT and heterogeneous simulations under both the steady state and transient conditions, as shown in Figures 5 and 6, respectively. The mass distributions in the mobile and immobile zones of the homogeneous MRMT systems and mass distributions in the coarse materials (gravel and sand) and the finer materials (silty sand and clay) of the heterogeneous systems were then evaluated separately. The mass residing in the mobile and immobile zones of the homogeneous MRMT and heterogeneous scenarios are plotted in Figure 9a for the steady state simulations (S1) and in Figure 9b for the transient simulations (S2) after pumping started. The mass in the clay and silty sand of the heterogeneous scenarios was compared to the mass in the immobile zones of the homogeneous MRMT scenarios. All contaminants were initially placed in the mobile zone in the homogenous-MRMT simulation and in the coarse materials in the heterogeneous simulation and declined rapidly in the first few years (Figure 9a). Despite the decline in mass in both the mobile zone of the homogeneous MRMT simulation and the coarse materials of the heterogeneous simulation, the mass of the homogeneous MRMT simulation drops to much lower values compared to the mass of the heterogeneous simulation. The mass differences between the homogeneous MRMT and heterogeneous simulations under transient conditions (Figure 9b) are larger than the mass differences observed in the simulations under steady state conditions. For further details, the mass distributions in the different phases (mobile and immobile zones of the homogeneous MRMT simulation and the coarse materials and clay of the heterogeneous simulation) are plotted separately in Figures S7 and S8.

In our implementation of the MRMT method, multiple calibrations were conducted by varying the capacity coefficients (treating either clay or clay and silt as the immobile zone) and the mass transfer rates to fit the tailings, and the mass distributions for the homogeneous MRMT and heterogeneous simulations were compared for each calibration. The results of the calibration that generated the closest tails and mass distributions of the homogeneous MRMT simulations to those of the heterogeneous simulations are presented in Figures 2 and S2, respectively. The late-time tails generated by the MRMT simulations fit the corresponding tails of the heterogeneous simulations well under steady state flow conditions. The mass in the mobile zone

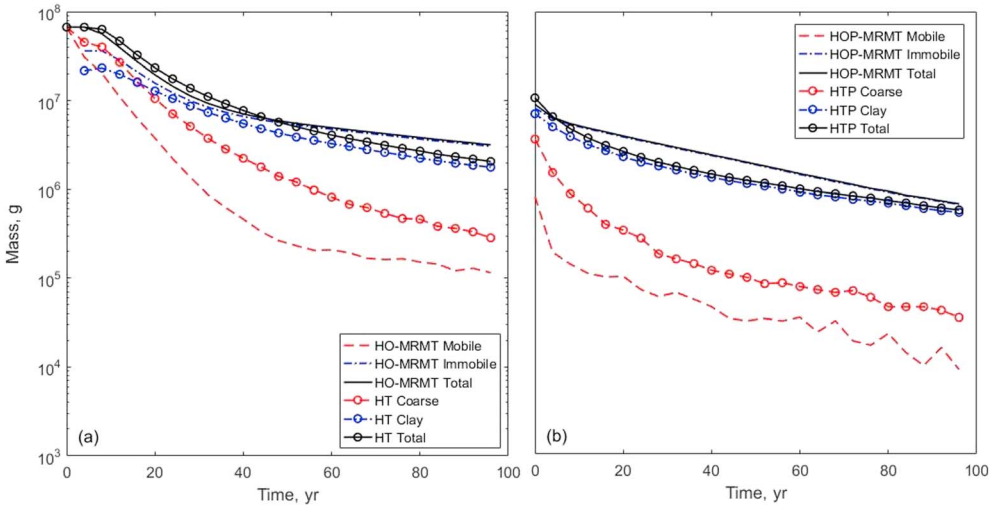

Figure 9. Time continuous mass change for the homogeneous MRMT and heterogeneous simulations. (a): Steady state. The mass decline in the mobile zone of the homogeneous MRMT simulation and in the coarse materials of the heterogeneous simulation and mass increases in the immobile zones of the homogeneous MRMT simulation and in the clay of the heterogeneous simulation happen in the first few years, which are not clearly visible on the plot; (b): after pumping is started, HO-MRMT and HT refer to the homogeneous MRMT and heterogeneous results under steady state conditions, respectively. HOP-MRMT and HTP refer to the homogeneous MRMT and heterogeneous results under transient conditions, respectively. MRMT = multirate mass transfer.

of the homogeneous MRMT simulations, however, is always lower than the mass in the coarse materials of the heterogeneous simulations, which likely augments the differences in the tails under transient boundary conditions. Therefore, identifying the time-varying mass in the mobile and immobile zones is considered a potential way to capture the tails of the heterogeneous simulations under different boundary conditions. However, no previous research that determines the mass or concentration separately for mobile and immobile zones was found. Instead, previously reported studies only examined the residence concentrations or flux-averaged concentrations in mobile zones (e.g., Haggerty & Gorelick, 1995; Haggerty et al., 2004; Harvey & Gorelick, 2000; Silva et al., 2009). Hence, simulating the mass in both the mobile and immobile zones accurately could be vital to represent the transport process under transient flow conditions in future studies.

4.2. Ergodicity and Effects of the Local Versus Regional Changes in the Flow System

Previous work on MRMT methods (e.g., Pedretti et al., 2014) has raised the issue of ergodicity, wherein the scale of the transport processes may be too local to sufficiently "sample" enough of the heterogeneity to reach the asymptotic conditions that can be considered generally representative. An important difference between the random fields of Pedretti et al. (2014) and those of this study is that while ours consist mainly of aquifer-aquitard complexes, Pedretti et al.'s consist entirely of the heterogeneity within the aquifer materials modeled as Gaussian random fields. In the latter, the modeled plumes must indeed encounter enough of the aquifer heterogeneity to approach asymptotic conditions. In the hydrofacies-based aquifer-aquitard random fields generated with T-PROGS of this paper, however, the main features producing dispersion are the nearly ubiquitously interconnected (percolating) aquifer facies and the omnipresent, adjacent aquitard facies. Because of the ubiquitously percolating aquifer facies, as found by LaBolle and Fogg (2001), the modeled plumes in a system such as that of this study behave very consistently from realization to realization, and the transport phenomena are consistent at most scales and localities, with relatively rapid transport in the interconnected aquifers together with ubiquitous mass transfer to and from the aquitard units. In fact, LaBolle and Fogg (2001) noted that in such a system, asymptotic conditions may never be reached, and the researchers suggested these transport phenomena as explanations of the strong scale dependence of the apparent dispersivities.

Accordingly, we do not anticipate that the nonergodicity bears heavily on the generality of our modeling results. Nevertheless, one might argue that our well boundary conditions are sufficiently local within the

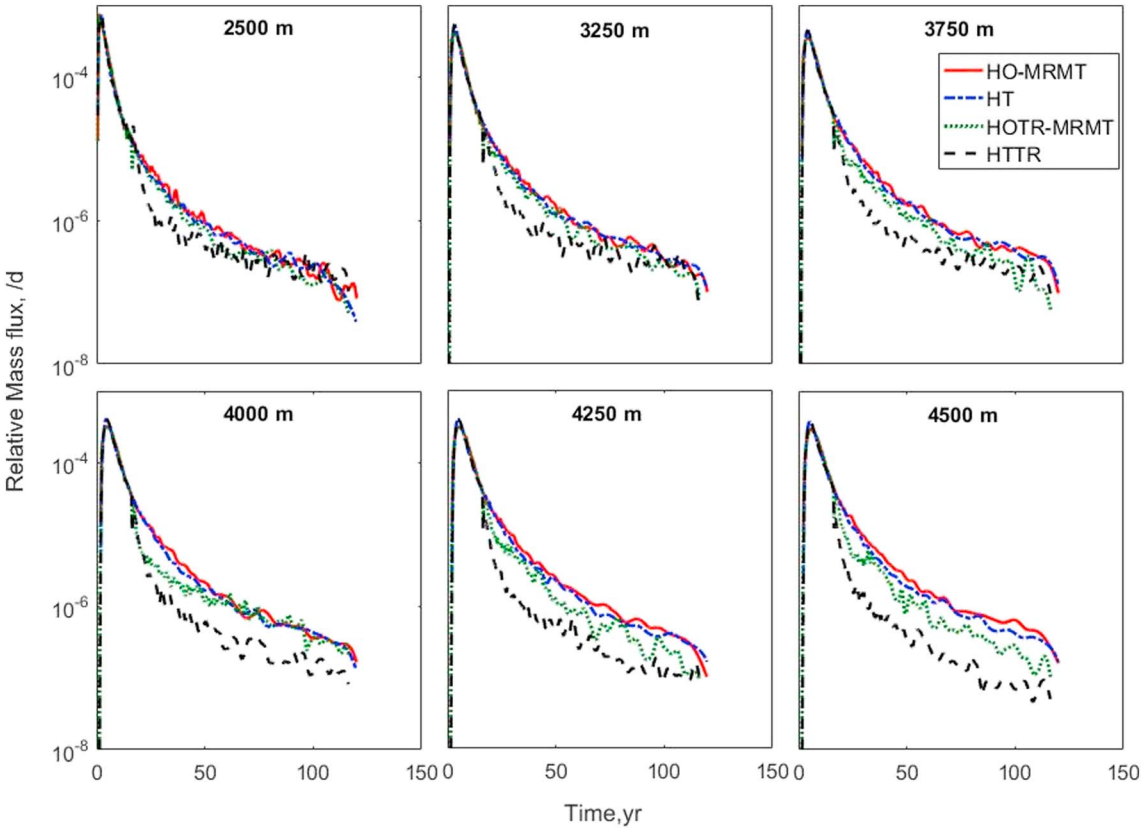

Figure 10. Breakthrough curves for control planes at different locations: x = 2,500, 3,250, 3,750, 4,000, 4,250, and 4,500 m, which includes 5.3, 8.0, 9.8, 10.7, 11.6, and 12.5 mean lengths, respectively. HO-MRMT and HT refer to the homogeneous and heterogeneous results under steady state conditions, respectively. HOTR-MRMT and HTTR refer to the homogeneous and heterogeneous results under transient boundary conditions, respectively.

heterogeneous fields that the nonergodic effects could be of concern related to which facies those wells penetrate in the individual realizations. Therefore, we ran additional scenarios in which the forcings that produce the regional flow and the transients are regional forcings, rather than those from wells. In these other scenarios (S3), rather than pumping from wells as in scenario S2, we introduced a transient representing a change from purely horizontal flow to predominantly vertical flow with a vertical component representing the effects of recharge from above and flow out of the bottom of the model into deeper parts of the aquifer system (see the description in the methods section). The results are shown in Figure 10. Significant reductions in the mass fluxes were observed for the heterogeneous simulation (HTTR) after the flow field was changed due to varied boundary conditions. However, for the homogeneous MRMT simulation (HOTR-MRMT), the changes in the mass fluxes across the control planes were not as significant as those in the heterogeneous simulations because of the unvaried mass transfer rates between the mobile and immobile zones. The mismatches between the tails of the homogeneous MRMT and heterogeneous simulations are observed for all control planes that are located at distances including 5 to 12 correlation scales.

In transient scenario S2, the boundary condition change was induced by the initiation of pumping at the local scale. Because the lateral extents of the pumping well drawdowns are only 2 to 5 times larger than the maximum facies correlation length of 280 m, there may be the potential for an effect due to nonergodicity, where local effects of the heterogeneity are unique to particular realizations. In scenario S3, transient conditions were simulated with a regional-scale change in the flow field by applying recharge and a vertical gradient. The mismatches between the tails of the heterogeneous and homogeneous simulations are observed in all control planes that cover 5–13 times the correlation length. This result is consistent with observations from previous experiments involving pumping wells,

indicating that the failure of the MRMT model under transient boundary conditions is not an artifact of nonergodicity.

In a stratified alluvial aquifer, the horizontal hydraulic gradients are commonly on the order of 10^{-3}, and the vertical gradients tend to be larger owing to the relatively low, effective K and the combination of recharge at the water table and pumpage at depth (e.g., Fogg, 1986). When the pumping and recharge fluctuate, the vertical gradients can easily fluctuate between values that are 10 to 1,000 times higher than the horizontal gradients. This situation will result in significantly increased vertical leakage rates and mass transfer rates into and out of the aquitards. This phenomenon explains why in scenario S3 when the vertical hydraulic gradients were increased, the changes in the x, y, and z directions were observed in Figure 10. Basically, the 3-D flow fields create mass transfer rates among the facies that are functions of both diffusion and slow advection. Because of the varied mass transfer rates among the facies due to the change in the boundary condition, the MRMT models that work under steady state conditions with unvaried mass transfer rates between the immobile and mobile zones will fail to represent the transport under transient conditions. Therefore, upscaled models that can represent transient transport, including different boundary conditions at regional scales, are needed.

4.3. Other Potential Problems Applying the MRMT Method

The homogeneous MRMT simulations also failed to reproduce the high concentrations that were observed for the heterogeneous simulations as the plume migrated with time. The uneven distributions of the concentration with the location are the result of the permeability heterogeneity in the heterogeneous simulations. With a uniformity of the flow field in the homogenous domain, reproducing these high concentrations will also be an important task during the upscaling of the transport process as in real fields since the maximum detected concentration is also an important indicator for site management.

The results shown in this study indicate errors of 1–2 orders of magnitude in the concentration or mass flux between the homogeneous MRMT and heterogeneous simulations, which resulted from only one set of pumping wells and simple changes in the boundary conditions. However, in the real field, there would be more complex, transient conditions at the regional scale, where more wells are used, thus resulting in more changes in pumping, more recharge, and more complex source loading, such as nonpoint sources. These factors would cause additional uncertainties and perturbations on the upscaled model. The performance of the MRMT model for representing these transient transport processes needs to be evaluated, especially in complex nonpoint source scenarios.

4.4. Implications for the Application of Other Nonlocal Methods for Upscaling Transport

Other nonlocal methods, such as CTRW and fADE (Benson et al., 2000a, 2000b; Berkowitz et al., 2006; Berkowitz & Scher, 1995, 1998), have been demonstrated to represent non-Fickian transport with steady state boundary conditions in field and laboratory work. Given that the application of these methods also requires the calibration of parameters to fit plume migration and mass distributions under steady state conditions, we anticipate that these methods will suffer from the same errors when the boundary conditions shift significantly enough to change the internal hydraulic gradients among the hydrofacies, thereby changing the mass transfer rates and consequences. Cortis and Knudby (2006) applied CTRW to a transient flow problem with fixed boundary conditions, which showed possible implications for the interpretation of pumping test data. The researchers were able to do the aforementioned by changing the CTRW parameters with time and distance as a function of the changing velocity field under transient conditions. However, their approach does not present a method that is sufficiently general to a priori estimate those parameters unless one already has BTCs to guide the fitting procedure. After changing the boundary conditions, such as the mass loading functions or pumping wells, the model with previously determined parameters can be expected to fail to represent the transport processes. Therefore, even though the CTRW could presumably work well using a time-dependent memory function, the method still needs a predetermined function that varies with time, which has not been found in any studies that show how this function can be estimated. fADE is a special case of CTRW, whose mathematical similarity has been discussed in Berkowitz et al. (2006) and Metzler and Klafter (2000). Therefore, we see no reason for fADE to perform any better for transport behaviors under transient boundary conditions.

5. Summary and Conclusions

This research studied a previously developed upscaling approach, the MRMT method, to represent solute transport under both steady state and transient flow conditions. For forward plume movement under steady state conditions, MRMT can capture the early- and late-time tails quite well. When the boundary conditions change due to the introduction of pumping wells, however, the MRMT model no longer represents the effects of heterogeneity on transport. The potential causes of the misrepresentation with variable boundary conditions, such as variable mass transfer and mass distributions, were investigated. The results from scenarios with local and regional changes of the flow fields indicate the significant impacts of variable flow fields, which result in changes in the mass transfer processes of the transport. The pervasively interconnected (percolating) nature of our modeled aquifer/aquitard complexes that are modeled as hydrofacies, together with the similar failure of the MRMT model when the boundary condition forcings are regional rather than locally induced by pumping wells, indicate that the results are general and not artifacts of nonergodic problems. The mass transfer between the mobile and immobile zones is strongly affected by the internal hydraulic gradients between the high- and low-K materials. When the boundary conditions change, these hydraulic gradients and in turn the mass transfer phenomena change, thereby rendering the upscaled MRMT model ineffective for modeling transport. Additionally, the quantities of mass in the mobile and immobile zones of the homogeneous MRMT simulations differ significantly from those in the coarse and finer materials in the heterogeneous simulations. Under transient conditions, the disparities are even larger, which may contribute to the failure of fitting the tails for the homogeneous MRMT and heterogeneous simulations. The homogeneous MRMT simulations also failed to capture the maximum concentrations that were observed for the heterogeneous simulations, which can result in misguidance for site management when local concentrations are monitored. Moreover, in realistic settings, especially in the case of an intensely irrigated agriculture basin, contamination sources are often characterized as nonpoint sources. Thus, the behaviors of the phenomena discussed in this study need to be explored for nonpoint source cases.

Therefore, under the circumstances of 3-D heterogeneous flow systems and transient flow fields caused by transient boundary conditions, the MRMT method shows poor applicability. The same appears to be true for other transport upscaling methods. To accommodate the needs for regional-scale transport and local site management, a method that can represent plume movement, especially capture late-time tails, in heterogeneous systems under transient conditions is needed.

Acknowledgments
This research was supported by the U.S. Department of Energy, Cerc-Wet program. Data used in this work are available at the website (https://doi.org/10.15146/R3NM3S).

References

Anastasiadis, P. (2004). Evaluating non-point source pollution using GIS. *Fresenius Environmental Bulletin*, *13*(11A), 1168–1172.

Belitz, K., Phillips, S. P., & Gronberg, J. M. (1993). *Numerical simulation of ground-water flow in the central part of the Western San Joaquin Valley*, *Water-Supply Paper* (Vol. 2396, p. 69). California: U.S. Geological Survey.

Benson, D. A., Schumer, R., Meerschaert, M. M., & Wheatcraft, S. W. (2001). Fractional dispersion, Lévy motion, and the MADE tracer tests. *Transport in Porous Media*, *42*(1/2), 211–240. https://doi.org/10.1023/A:1006733002131

Benson, D. A., Wheatcraft, S. W., & Meerschaert, M. M. (2000a). The fractional-order governing equation of Lévy motion. *Water Resources Research*, *36*(6), 1413–1423. https://doi.org/10.1029/2000WR900032

Benson, D. A., Wheatcraft, S. W., & Meerschaert, M. M. (2000b). Application of a fractional advection–dispersion equation. *Water Resources Research*, *36*(6), 1403–1412. https://doi.org/10.1029/2000WR900031

Berkowitz, B., Cortis, A., Dentz, M., & Scher, H. (2006). Modeling non-Fickian transport in geological formations as a continuous time random walk. *Reviews of Geophysics*, *44*, RG2003. https://doi.org/10.1029/2005RG000178

Berkowitz, B., & Scher, H. (1995). On characterization of anomalous dispersion in porous and fractured media. *Water Resources Research*, *31*(6), 1461–1466. https://doi.org/10.1029/95WR00483

Berkowitz, B., & Scher, H. (1998). Theory of anomalous chemical transport in random fracture networks. *Physical Review E*, *57*(5), 5858–5869. https://doi.org/10.1103/PhysRevE.57.5858

Bianchi, M., Zheng, C., Wilson, C., Tick, G. R., Liu, G., & Gorelick, S. M. (2011). Spatial connectivity in a highly heterogeneous aquifer: From cores to preferential flow paths. *Water Resources Research*, *47*, W05524. https://doi.org/10.1029/2009WR008966

Boso, F., Bellin, A., & Dumbser, M. (2012). Numerical simulations of solute transport in highly heterogeneous formations: A comparison of alternative numerical schemes. *Advances in Water Resources*, *52*, 178–189. https://doi.org/10.1016/j.advwatres.2012.08.006

Brusseau, M. L., & Guo, Z. (2014). Assessing contaminant-removal conditions and plume persistence through analysis of data from long-term pump-and-treat operations. *Journal of Contaminant Hydrology*, *164*, 16–24. https://doi.org/10.1016/j.jconhyd.2014.05.004

Brusseau, M. L., Hatton, J., & DiGuiseppi, W. (2011). Assessing the impact of source-zone remediation efforts at the contaminant-plume scale through analysis of contaminant mass discharge. *Journal of Contaminant Hydrology*, *126*(3-4), 130–139. https://doi.org/10.1016/j.jconhyd.2011.08.003

Brusseau, M. L., Nelson, N. T., Zhang, Z., Blue, J. E., Rohrer, J., & Allen, T. (2007). Source-zone characterization of a chlorinated-solvent contaminated superfund site in Tucson, AZ. *Journal of Contaminant Hydrology*, *90*(1-2), 21–40. https://doi.org/10.1016/j.jconhyd.2006.09.004

Carle, S. F. (1997). Implementation schemes for avoiding artifact discontinuities in simulated annealing. *Mathematical Geology*, *29*(2), 231–244. https://doi.org/10.1007/BF02769630

Carle, S. F., & Fogg, G. E. (1996). Transition probability-based indicator geostatistics. *Mathematical Geology*, *28*(4), 453–476. https://doi.org/10.1007/BF02083656

Carle, S. F., & Fogg, G. E. (1997). Modeling spatial variability with one- and multi-dimensional continuous Markov chains. *Mathematical Geology*, *29*(7), 891–918. https://doi.org/10.1023/A:1022303706942

Carle, S. F., LaBolle, E. M., Weissmann, G. S., Van Brocklin, D., & Fogg, G. E. (1998). Conditional simulation of hydrofacies architecture: A transition probability/Markov chain approach. In G. S. Fraser, & J. M. Davis (Eds.), *Hydrogeologic Models of Sedimentary Aquifers*, *Concepts Hydrogeol. Environ. Geol. Ser.* (Vol. 1, pp. 147–170). Tulsa, OK: Society for Sedimentary Geology.

Carrera, J., & Neuman, S. P. (1986). Estimation of aquifer parameters under transient and steady-state conditions. 1. Maximum likelihood method incorporating prior information. *Water Resources Research*, *22*(2), 199–210. https://doi.org/10.1029/WR022i002p00199

Carrera, J., Sanchez-Vila, X., Benet, I., Medina, A., Galarza, G., & Guimera, J. (1998). On matrix diffusion: formulations, solution methods and qualitative effects. *Hydrogeology Journal*, *6*(1), 178–190. https://doi.org/10.1007/s100400050143

Cassiraga, E. F., Fernàndez-Garcia, D., & Gómez-Hernández, J. J. (2005). Performance assessment of solute transport upscaling methods in the context of nuclear waste disposal. *International Journal of Rock Mechanics and Mining Sciences*, *42*(5–6), 756–764. https://doi.org/10.1016/j.ijrmms.2005.03.013

Chae, G. T., Kim, K. J., Yun, S. T., Kim, K. H., Kim, S. O., Choi, B. Y., et al. (2004). Hydrogeochemistry of alluvial ground-waters in an agricultural area: An implication for groundwater contamination susceptibility. *Chemosphere*, *55*(3), 369–378. https://doi.org/10.1016/j.chemosphere.2003.11.001

Cortis, A., & Berkowitz, B. (2005). Computing "anomalous" contaminant transport in porous media: The CTRW Matlab toolbox. *Ground Water*, *43*(6), 947–950. https://doi.org/10.1111/j.1745-6584.2005.00045.x

Cortis, A., & Knudby, C. (2006). A continuous time random walk approach to transient flow in heterogeneous porous media. *Water Resources Research*, *42*, W10201. https://doi.org/10.1029/2006WR005227

Dagan, G. (1994). Upscaling of dispersion coefficients in transport through heterogeneous formations. *Comput Methods Water Resour X*, *1*, 431–439.

Dagan, G., & Lessoff, S. C. (2001). Solute transport in heterogeneous formations of bimodal conductivity distribution. 1. Theory. *Water Resources Research*, *37*(3), 465–472. https://doi.org/10.1029/2000WR900225

Dearden, R. A., Noy, D. J., Lelliott, M. R., Wilson, R., & Wealthall, G. P. (2013). Release of contaminants from a heterogeneously fractured low permeability unit underlying a DNAPL source zone. *Journal of Contaminant Hydrology*, *153*, 141–155.

Dubrovsky, N. M., Kratzer, C. R., Brown, L. R., Gronberg, J. M., & Burow, K. R. (1998). Water quality in the San Joaquin-Tulare Basins, California, 1992–95, U.S. Geol. Surv. Circ. 1159, 38 pp.

Fernàndez-Garcia, D., & Gómez-Hernández, J. J. (2007). Impact of upscaling on solute transport: travel times, scale dependence of dispersivity, and propagation of uncertainty. *Water Resources Research*, *43*, W02423. https://doi.org/10.1029/2005WR004727

Fernàndez-Garcia, D., Illangasekare, T. H., & Rajaram, H. (2005). Differences in the scale dependence of dispersivity estimated from temporal and spatial moments in chemically and physically heterogeneous porous media. *Advances in Water Resources*, *28*(7), 745–759. https://doi.org/10.1016/j.advwatres.2004.12.011

Fernàndez-Garcia, D., Llerar-Meza, G., & Gómez-Hernández, J. J. (2009). Upscaling transport with mass transfer models: Mean behavior and propagation of uncertainty. *Water Resources Research*, *45*, W10411. https://doi.org/10.1029/2009WR007764

Fleckenstein, J. H., & Fogg, G. E. (2008). Efficient upscaling of hydraulic conductivity in heterogeneous alluvial aquifers. *Hydrogeology Journal*, *16*(7), 1239–1250. https://doi.org/10.1007/s1004000803123

Fogg, C. E., Carle, S. F., & Green, C. (2000). Connected-network paradigm for the alluvial aquifer system. In D. Zhang & C. L. Winter (Eds.), *Theory, Modeling, and Field Investigation in Hydrogeology: A Special Volume in Honor of Shlomo P. Neuman's 60th Birthday*, *Special Paper* (Vol. 348, pp. 25–42). Boulder, CO: Geological Society of America. https://doi.org/10.1130/0-8137-2348-5.25

Fogg, G. E. (1986). Groundwater flow and sand body interconnectedness in a thick, multiple-aquifer system. *Water Resources Research*, *22*(5), 679–694. https://doi.org/10.1029/WR022i005p00679

Fogg, G. E., & LaBolle, E. M. (2006). Motivation of synthesis, with an example on groundwater quality sustainability. *Water Resources Research*, *42*, W03S05. https://doi.org/10.1029/2005WR004372

Fogg, G. E., LaBolle, E. M., & Weissmann, G. S. (1999). Groundwater vulnerability assessment: Hydrogeologic perspective and example from Salinas Valley, California. In D. L. Corwin, K. Loague, & T. R. Ellsworth (Eds.), *Assessment of Non-point Source Pollution in the Vadose Zone*, *Geophysical Monograph Series* (Vol. 108, pp. 45–61). Washington, DC: American Geophysical Union. https://doi.org/10.1029/GM108p0045

Fogg, G. E., & Zhang, Y. (2016). Debates—Stochastic subsurface hydrology from theory to practice: A geologic perspective. *Water Resources Research*, *52*, 9235–9245. https://doi.org/10.1002/2016WR019699

Gailey, R. (2018). Using geographic distribution of well-screen depths and hydrogeologic conditions to identify areas of concern for contaminant migration through inactive supply wells. *Hydrogeology Journal*, *26*(6), 2071–2088. https://doi.org/10.1007/s10040-018-1734-1

Guo, Z., & Brusseau, M. L. (2017). The impact of well-field configuration and permeability heterogeneity on contaminant mass removal and plume persistence. *Journal of Hazardous Materials*, *333*, 109–115. https://doi.org/10.1016/j.jhazmat.2017.03.012

Guo, Z., Fogg, G. E., Brusseau, M. L., LaBolle, E. M., & Lopez, J. (2019). Modeling groundwater contaminant transport in the presence of large heterogeneity: a case study comparing MT3D and RWhet. *Hydrogeology Journal*, *27*, 1363–1371.

Guswa, A. J., & Freyberg, D. L. (2000). Slow advection and diffusion through low permeability inclusions. *Journal of Contaminant Hydrology*, *46*(3–4), 205–232. https://doi.org/10.1016/S0169-7722(00)00136-4

Haggerty, R., & Gorelick, S. M. (1995). Multiple-rate mass transfer for modeling diffusion and surface reactions in media with pore-scale heterogeneity. *Water Resources Research*, *31*(10), 2383–2400. https://doi.org/10.1029/95WR10583

Haggerty, R., Harvey, C. F., Freiherr von Schwerin, C., & Meigs, L. C. (2004). What controls the apparent timescale of solute mass transfer in aquifers and soils? A comparison of experimental results. *Water Resources Research*, *40*, W01510. https://doi.org/10.1029/2002WR001716

Harbaugh, A. W., Banta, E. R., Hill, M. C., & McDonald, M. G. (2000). MODFLOW-2000, The U.S. Geological Survey modular ground-water model-user guide to modularization concepts and the ground-water flow process, U.S. Geological Survey Open-File Report 00-92, 2000.

Harter, T., J. R. Lund, J. Darby, G. E. Fogg, R. Howitt, K. K. Jessoe, et al., 2012. Addressing Nitrate in California's Drinking Water With A Focus on Tulare Lake Basin and Salinas Valley Groundwater, Report for the State Water Resources Control Board Report to the Legislature, Center for Watershed Sciences, University of California, Davis, 87p.

Harvey, C., & Gorelick, S. M. (2000). Rate-limited mass transfer or macrodispersion: Which dominates plume evolution at the Macrodispersion Experiment (MADE) site? *Water Resources Research*, *36*(3), 637–650. https://doi.org/10.1029/1999WR900247

Henri, C. V., & Fernàndez-Garcia, D. (2014). Toward efficiency in heterogeneous multispecies reactive transport modeling: A particle-tracking solution for first-order network reactions. *Water Resources Research*, *50*, 7206–7230. https://doi.org/10.1002/2013WR014956

Henri, C. V., & Fernàndez-Garcia, D. (2015). A random walk solution for modeling solute transport with network reactions and multi-rate mass transfer in heterogeneous systems: Impact of biofilms. *Advances in Water Resources*, *86*, 199–132.

LaBolle, E. M., & Fogg, G. E. (2001). Role of molecular diffusion in contaminant migration and recovery in an alluvial aquifer system. *Transport in Porous Media*, *42*(1/2), 155–179. https://doi.org/10.1023/A:1006772716244

Li, L., Zhou, H., & Gómez-Hernández, J. J. (2011). Transport upscaling using multi-rate mass transfer in three-dimensional highly heterogeneous porous media. *Advances in Water Resources*, *34*(4), 478–489. https://doi.org/10.1016/j.advwatres.2011.01.001

Lichtner, P. C., Kelkar, S., & Robinson, B. (2002). New form of dispersion tensor for axisymmetric porous media with implementation in particle tracking. *Water Resources Research*, *38*(8), 1146. https://doi.org/10.1029/2000WR000100

Matthieu, D. E. III, Brusseau, M. L., Guo, Z., Plaschke, M., Carroll, K. C., & Brinker, F. (2014). Persistence of a groundwater contaminant plume after hydraulic source containment at a chlorinated-solvent contaminated site. *Groundwater Monitoring and Remediation*, *34*(4), 23–32. https://doi.org/10.1111/gwmr.12077

McDonald, M. G., & Harbaugh, A. W. (1988). A modular three-dimensional finite-difference ground-water flow model. U.S. Geological Survey Techniques of Water-Resources Investigations. Chapter A1, 586 p.

Metzler, R., & Klafter, J. (2000). The random walk's guide to anomalous diffusion: a fractional dynamics approach. *Physics Reports*, *339*(1), 1–77.

Nativ, R. (2004). Can the desert bloom? Lessons learned from the Israeli case. *Ground Water*, *42*(5), 651–657. https://doi.org/10.1111/j.1745-6584.2004.tb02719.x

Nkedi-Kizza, P., Biggar, J. W., Selim, H. M., Van Genuchten, M. T., Wierenga, P. J., Davidson, J. M., & Nielsen, D. R. (1984). On the equivalence of two conceptual models for describing ion exchange during transport through an aggregated oxisol. *Water Resources Research*, *20*(8), 1123–1130. https://doi.org/10.1029/WR020i008p01123

Nolan, B. T., Hitt, K. J., & Ruddy, B. C. (2002). Probability of nitrate contamination of recently recharged groundwaters in the conterminous United States. *Environmental Science & Technology*, *26*(10), 2138–2145. https://doi.org/10.1021/es0113854

Pedretti, D., & Fernandez-Garcia, D. (2013). An automatic locally-adaptive method to estimate heavily-tailed breakthrough curves from particle distributions. *Advances in Water Resources*, *59*, 52–65. https://doi.org/10.1016/j.advwatres.2013.05.006

Pedretti, D., Fernandez-Garcia, D., Sanchez-Vila, X., Bolster, D., & Benson, D. A. (2014). Apparent directional mass-transfer capacity coefficients in three-dimensional anisotropic heterogeneous aquifers under radial convergent transport. *Water Resources Research*, *50*, 1205–1224. https://doi.org/10.1002/2013WR014578

Renard, P., & de Marsily, G. (1997). Calculating equivalent permeability: A review. *Advances in Water Resources*, *20*(5–6), 253–278. https://doi.org/10.1016/S0309-1708(96)00050-4

Rubin, Y., Sun, A., Maxwell, R., & Bellin, A. (1999). The concept of block-effective macrodispersivity and a unified approach for grid-scale- and plume-scale dependent transport. *Journal of Fluid Mechanics*, *395*, 161–180. https://doi.org/10.1017/S0022112099005868

Salamon, P., Fernàndez-Garcia, D., & Gómez-Hernández, J. J. (2006). Modeling mass transfer processes using random walk particle tracking. *Water Resources Research*, *42*, W11417. https://doi.org/10.1029/2006WR004927

Sanchez-Vila, X., Guadagnini, A., & Carrera, J. (2006). Representative hydraulic conductivities in saturated groundwater flow. *Reviews of Geophysics*, *44*, RG3002. https://doi.org/10.1029/2005RG000169

Scheibe, T., & Yabusaki, S. (1998). Scaling of flow and transport behavior in heterogeneous groundwater systems. *Advances in Water Resources*, *22*(3), 223–238. https://doi.org/10.1016/S0309-1708(98)00014-1

Seyedabbasi, M. A., Newell, J. C., Adamson, D. T., & Sale, T. C. (2012). Relative contribution of DNAPL dissolution and matrix diffusion to the long-term persistence of chlorinated solvent source zones. *Journal of Contaminant Hydrology*, *134*, 69–81. https://doi.org/10.1016/j.jconhyd.2012.03.010

Silva, O., Carrera, J., Kumar, S., Dentz, M., Alcolea, A., & Willmann, M. (2009). A general real-time formulation for multi-rate mass transfer problems. *Hydrology and Earth System Sciences*, *6*(2), 2415–2449. https://doi.org/10.5194/hessd-6-2415-2009

Styles, S. W., & Burt, C. M. (1999). Subsurface flows water balance components for irrigation district in San Joaquin Valley. Conference on Benchmarking irrigation system performance using water measurement and water balances. San Luis Obispo, CA. ITRC Paper 99-002.

Tompson, A. F. B., Carle, S. F., Rosenberg, N. D., & Maxwell, R. M. (1999). Analysis of groundwater migration from artificial recharge in a large urban aquifer: A simulation perspective. *Water Resources Research*, *35*(10), 2981–2998. https://doi.org/10.1029/1999WR900175

Vengosh, A., Gill, J., Davisson, M. L., & Hudson, G. B. (2002). A multi-isotope (B, Sr, O, H, and C) and age dating (^{3}H–^{3}He and ^{14}C) study of groundwater from Salinas Valley, California: Hydrochemistry, dynamics, and contamination processes. *Water Resources Research*, *38*(1), 1008. https://doi.org/10.1029/2001WR000517

Weissmann, G. S., Yong, Z., LaBolle, E. M., & Fogg, G. E. (2002). Dispersion of groundwater age in an alluvial aquifer system. *Water Resources Research*, *38*(10), 1198. https://doi.org/10.1029/2001WR000907

Wen, X. H., & Gómez-Hernández, J. J. (1996). Upscaling hydraulic conductivities: An overview. *Journal of Hydrology*, *183*(1–2), ix–xxxii.

Willmann, M., Carrera, J., & Sánchez-Vila, X. (2008). Transport upscaling in heterogeneous aquifers: What physical parameters control memory functions? *Water Resources Research*, *44*, W12437. https://doi.org/10.1029/2007WR006531

Zektser, I. S., & Everett, L. G. (Eds.) (2004). Groundwater resources of the world and their use, UNESCO IHP-VI Series on Groundwater No. 6. Paris.

Zhang, H., Harter, T., & Sivakumar, B. (2006). Nonpoint source solute transport normal to aquifer bedding in heterogeneous, Markov chain random fields. *Water Resources Research*, *42*, W06403. https://doi.org/10.1029/2004WR003808

Zhang, Y., Benson, D. A., Meerschaert, M. M., & LaBolle, E. M. (2007). Space-fractional advection–dispersion equations with variable parameters: diverse formulas, numerical solutions, and application to the macrodispersion experiment site data. *Water Resources Research*, *43*, W05439. https://doi.org/10.1029/2006WR004912

Zhang, Z., & Brusseau, M. L. (1998). Characterizing three-dimensional hydraulic conductivity distributions using qualitative and quantitative geologic borehole data: Application to a field site. *Ground Water*, *36*(4), 671–678. https://doi.org/10.1111/j.1745-6584.1998.tb02842.x

Zhang, Z., & Brusseau, M. L. (1999). Nonideal transport of reactive solutes in Heterogeneous porous media 5. Simulating regional-scale behavior of a trichloroethene plume during pump-and-treat remediation. *Water Resources Research*, *35*(10), 2921–2935.

Zhou, H., Li, L., & Gómez-Hernández, J. J. (2010). Three-dimensional hydraulic conductivity upscaling in groundwater modelling. *Computational Geosciences*, *36*(10), 1224–1235. https://doi.org/10.1016/j.cageo.2010.03.008

Zinn, B., & Harvey, C. F. (2003). When good statistical models of aquifer heterogeneity go bad: A comparison of flow, dispersion, and mass transfer in connected and multivariate gaussian hydraulic conductivity fields. *Water Resources Research*, *39*(3), 1051. https://doi.org/10.1029/2001WR001146